

Evolving Einstein’s Field Equations with Matter: The “Hydro without Hydro” Test

Thomas W. Baumgarte^{1,2}, Scott A. Hughes¹ and Stuart L. Shapiro^{1,2,3}

¹ *Department of Physics, University of Illinois at Urbana-Champaign, Urbana, IL 61801*

² *Department of Astronomy, University of Illinois at Urbana-Champaign, Urbana, IL 61801*

³ *NCSA, University of Illinois at Urbana-Champaign, Urbana, IL 61801*

We include matter sources in Einstein’s field equations and show that our recently proposed 3+1 evolution scheme can stably evolve strong-field solutions. We insert in our code known matter solutions, namely the Oppenheimer-Volkoff solution for a static star and the Oppenheimer-Snyder solution for homogeneous dust sphere collapse to a black hole, and evolve the gravitational field equations. We find that we can evolve stably static, strong-field stars for arbitrarily long times and can follow dust sphere collapse accurately well past black hole formation. These tests are useful diagnostics for fully self-consistent, stable hydrodynamical simulations in 3+1 general relativity. Moreover, they suggest a successive approximation scheme for determining gravitational waveforms from strong-field sources dominated by longitudinal fields, like binary neutron stars: approximate quasi-equilibrium models can serve as sources for the transverse field equations, which can be evolved without having to re-solve the hydrodynamical equations (“hydro without hydro”).

PACS numbers: 04.25.Dm, 04.30.Nk, 02.60.Jh

With the advent of gravitational-wave interferometry, the physics of compact objects is entering a particularly exciting phase. The new generation of gravitational-wave detectors, including LIGO, VIRGO, GEO and TAMA, may soon detect gravitational radiation directly for the first time, opening a gravitational-wave window to the Universe and making gravitational-wave astronomy a reality (see, *e.g.*, [1]).

To learn from such observations and to dramatically increase the likelihood of detection, one needs to predict the observed signal theoretically. Among the most promising sources are gravitational waves from the coalescences of black hole and neutron star binaries. Simulating such mergers requires self-consistent numerical solutions to Einstein’s field equations in three spatial dimensions plus time, which is extremely challenging. While several groups, including two “Grand Challenge Alliances” [2], have launched efforts to simulate compact binary coalescence (see also [3,4]), the problem is far from solved.

Many of the numerical codes, including those based on the ADM formulation of Einstein’s equations (after Arnowitt, Deser and Misner, [5]) develop instabilities and inevitably crash, even for small amplitude gravitational waves on a flat background (see, *e.g.*, [6]). To avoid this problem, several hyperbolic formulations have been developed [7], some of which have also been implemented numerically [8,9]. In a recent paper [10] (hereafter paper I), we have modified a formulation of Shibata and Nakamura [11], and have shown that our new formulation allows for stable, long-term evolution of gravitational waves. We pointed out its two advantages over many hyperbolic formulations: it requires far fewer equations and it does not require taking derivatives of the original 3+1 equations. The latter may be particularly important for

the evolution of matter sources, where matter derivatives could augment numerical error.

In this paper, we put matter sources into the field equations and test the evolution behavior for two known strong-field solutions: the Oppenheimer-Volkoff [12] solution for a static star, and the Oppenheimer-Snyder [13] solution for collapse of a homogeneous dust sphere to a black hole. We do not evolve the matter, but instead insert the known matter solutions into the numerically evolved field equations. This allows us to study hydrodynamical scenarios without re-solving hydrodynamical equations: “hydro without hydro”.

The purpose of this Brief Report and the hydro-without-hydro approach is twofold. First, we demonstrate that our evolution scheme can stably evolve strong-field solutions with matter sources. These calculations for strong longitudinal fields complement the tests for wave solutions (transverse fields) presented in paper I. This may be an important diagnostic for overcoming stability problems in relativistic hydrodynamical calculations (*cf.* [14] and discussion therein). Second, we demonstrate that we can integrate the field equations with *given* matter sources reliably. Specifically, we show that furnishing prescribed matter sources that already obey $\nabla \cdot \mathbf{T} = 0$ (where \mathbf{T} is the matter’s stress-energy tensor) rather than self-consistently evolving the matter together with the fields does not introduce instabilities. This decoupling (“hydro without hydro”) suggests new possibilities for determining gravitational waveforms emitted by, for example, inspiraling neutron stars binaries prior to reaching the innermost stable circular orbit by a successive approximation scheme.

In our formulation, we evolve the conformal metric $\tilde{\gamma}_{ij}$, the conformal exponent ϕ , the extrinsic curvature’s trace K and conformal trace-free part \tilde{A}_{ij} , and conformal con-

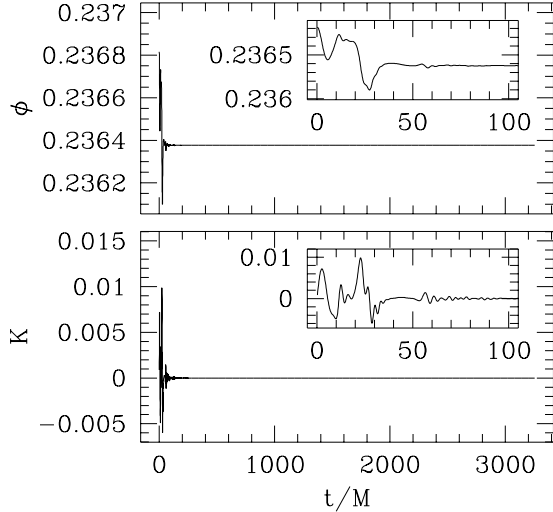


FIG. 1. Evolution of the conformal exponent ϕ and the trace of the extrinsic curvature K at the center for an OV static star (see text for details).

nection functions $\tilde{\Gamma}^i$. For the sake of brevity, we refer the reader to paper I for all field equations and their numerical implementation.

We first study the evolution of the gravitational fields for the Oppenheimer-Volkoff [12] solution of a relativistic, static star. We examine polytropic stellar models with equation of state $P = \kappa \rho_0^{1+1/n}$, focusing on polytropic index $n = 1$. Here P is the pressure and ρ_0 the rest-mass density; henceforth we set $G = 1 = c$, and we choose non-dimensional units in which $\kappa = 1$. We present results for a model with central density $\rho_0^c = 0.2$, for which the star has mass $M = 0.157$ and Schwarzschild radius $R = 0.866$. The small compaction, $R/M = 5.5$, indicates that the star is highly relativistic. The isotropic radius of this star is $\bar{R} = 0.7$. For comparison, the maximum mass configuration has a central density $\rho_0^c = 0.319$ and a mass $M = 0.164$.

We only evolve the gravitational fields, holding the matter sources to their OV values. We choose zero shift ($\beta^i = 0$) and set initial data for the lapse from the “Schwarzschild” lapse, α_{OV} . We evolve the lapse using harmonic slicing, which, for zero shift, reduces to $\partial_t \alpha = \partial_t e^{6\phi}$ (see, *e.g.*, paper I). We found that fixing the lapse to the exact solution $\alpha = \alpha_{OV}$ introduced instabilities, while integrating with harmonic slicing allowed stable evolutions while achieving the same lapse numerically. Note that the only non-vanishing matter sources appear in the evolution equation for K [*cf.* Eq. (15) of paper I]: the conformal splitting explicitly decouples transverse fields from static matter sources.

In Figure 1, we show K and ϕ for a long-term evolution. We used a $(32)^3$ grid and imposed the outer boundaries

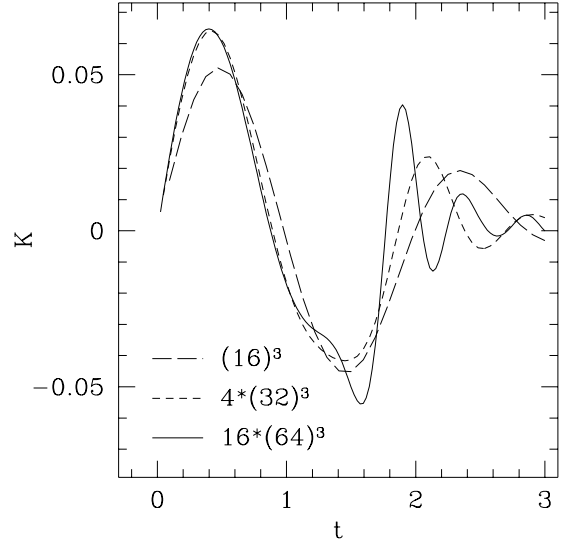


FIG. 2. Convergence test for K at the center. Note that the analytic solution is $K = 0$. The convergence of the scaled errors up to $t \sim 1$ indicates second order convergence of the code. The breakdown of second order convergence at later times is caused by effects of the surface of the star.

at $x, y, z = 2$. We terminated the calculation at $t = 512$ (corresponding to $t/M \sim 3255$), and found no evidence of an instability. Numerical noise develops during the early part of the evolution, but this noise propagates off the grid, and the evolution settles down into a numerical equilibrium solution.

The numerical noise originates from *three* sources: finite-difference error, noise from the surface of the star, and error due to imposing outer boundaries at finite distance. We now discuss these three sources in detail.

To check the local finite difference error, we perform a convergence test and evolve the same initial data on grids of $(16)^3$, $(32)^3$ and $(64)^3$ gridpoints, all with the outer boundary at $x, y, z = 3$. In Figure 2 we show results for K at the center from these runs. Note that the analytic solution is $K = 0$. We use second order accurate finite difference equations, and so expect error to decrease by a factor of four when doubling grid resolution. This behavior is seen at early times ($t \lesssim 1$) in Figure 2. There are deviations due to higher order error terms, but these decrease, and the scaled values of K converge to the second order error term.

At later times ($t \gtrsim 1$), second order convergence is spoiled by effects from the surface of the star. Note that the local speed of light at the center is $dr/dt \sim \alpha/e^{2\phi} \sim 0.36 < 1$. This delays signals from the surface, which otherwise would arrive at $t = \bar{r} = 0.7$. The code still converges, but no longer to second order. This effect is well known and appears in other simulations (compare, *e.g.*, [14]). Second-order spatial derivatives are not smooth at the star’s surface, so the finite-difference con-

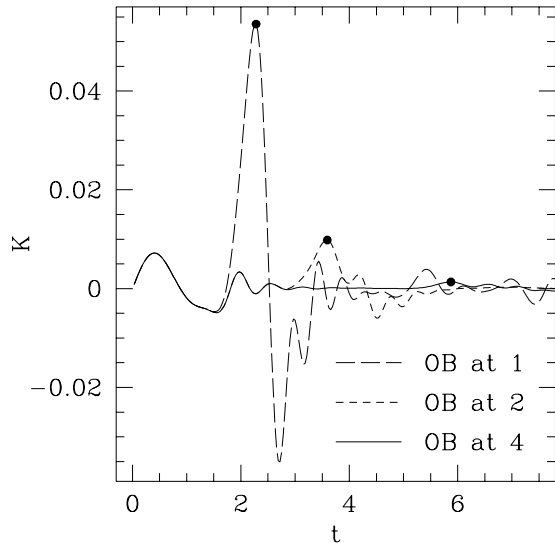


FIG. 3. Evolution of K at the center for different locations of the outer boundary. We double the number of gridpoints when doubling the distance to the outer boundary of the grid, so that the grid resolution remained constant. The dots mark the maximum error caused by the outer boundary.

vergence breaks down. We have run other cases with different stellar models (and radii) to show that this breakdown of second order convergence is due to errors originating at the star's surface.

Next we analyze the effect of the outer boundary (OB). We place the OB at $x, y, z = 1, 2$ and 4 , and run the code on grids of $(16)^3$, $(32)^3$ and $(64)^3$ gridpoints, so that the resolution of the star is constant. The results for K at the center are shown in Figure 3. As expected, all graphs agree until the center reaches the domain of dependence of the different OB locations. The run with the OB at 1 starts to deviate from the other two runs at $t \gtrsim 1$. At $t \gtrsim 2$ the run with OB at 2 starts to deviate from the run with OB at 4. The slight delay is again caused by the smaller value of the local speed of light toward the center of the star. The maximum error due to the OB (marked by dots in Figure 3) quickly decreases with larger OB location. Since our boundary conditions take into account the first order $(1/r)$ fall-off of the fields (see paper I), one would expect the error to scale with the square of the OB ratios, and hence with factors of at least four in our simulations. We find that the errors decrease by even slightly larger factors (5.4 and 7.2). For our resolution, the error is dominated by the local finite-differencing error even when the outer boundary is imposed at only a few stellar radii.

Going back to Figure 1, we can now identify the different sources of error in the early part of the evolution. The first peak in K around $t \sim 0.4 \sim 2.5M$ (see the panel in Figure 1) is caused by the local finite difference error. The next feature at $t \sim 2 \sim 12M$, with oscillations

at a higher frequency, originates from the surface of the star. The largest peak, at $t \sim 4 \sim 24M$, is caused by the outer boundary. Reflections of these errors off the OB reappear at later times, but ultimately propagate off the grid and leave behind a stable numerical equilibrium solution.

Turn now to an analysis of the gravitational fields associated with the collapse of a sphere of dust, Oppenheimer-Snyder collapse [13]. This configuration is highly dynamical — the matter very rapidly collapses to form a black hole. This case tests our ability to evolve into a very strong-field regime.

Again, we do not evolve the matter sources, but instead insert the exact solution for the matter (ρ , S_i , and S_{ij}) into the evolution code at each time step. The analytic solution for Oppenheimer-Snyder [13] collapse is transformed into maximal slicing and isotropic coordinates following [15]. This transformation involves only ordinary differential equations, which can be solved numerically. The lapse and shift corresponding to maximal slicing and isotropic coordinates are also obtained from this transformation and are inserted into the evolution code at each time step. Given the matter sources and the coordinate conditions, we independently evolve ϕ , $\tilde{\gamma}_{ij}$, \tilde{A}_{ij} , and $\tilde{\Gamma}^i$ with our 3+1 code. Having chosen maximal slicing, we can either set $K = 0$ or else evolve K dynamically and check that it indeed converges to zero.

We present results for a star that collapses from an initial Schwarzschild radius $R_{\text{star}} = 4M$ (or isotropic radius $\bar{R}_{\text{star}} = 2.94M$). The star collapses to a black hole and all of the matter has passed inside the event horizon by $t = 12.31M$. We terminate the evolution at $t = 17.39M$, the time up to which we have constructed exact data. The matter is so compact at the end ($\bar{R}_{\text{matter}} \simeq 0.14M$) that it is very poorly resolved on our 3-D grid. We impose the outer boundary conditions at $x = y = z = 4M$ (in isotropic coordinates), so that initially it is quite close to the star's surface.

In Figure 4, we show the evolution of the conformal exponent ϕ at the origin with $(16)^3$, $(32)^3$, and $(64)^3$ gridpoints and compare it with the exact solution. For this run, we evolved K . Figure 4 shows that the numerical evolution can follow the collapse well past black hole formation. The numerical solution converges to the exact solution (see especially the inner panel of Figure 4). At very late times, the grid resolution becomes increasingly poor, and ultimately convergence is spoiled by higher order finite difference errors. Up to these late times, the ADM and total rest mass are reliably conserved.

As with Oppenheimer-Volkoff stars, we find that non-smoothness of the gravitational fields at the surface spoils the second-order convergence of quantities in the domain of dependence of the surface. Here the effect is much stronger, since the matter density is non-zero all the way to the surface. However, we can lessen this effect and improve the behavior of the evolution by imposing the maximal slicing condition $K = 0$. This decouples the evolution equation for ϕ [cf. Eq. (14) of paper I] from the

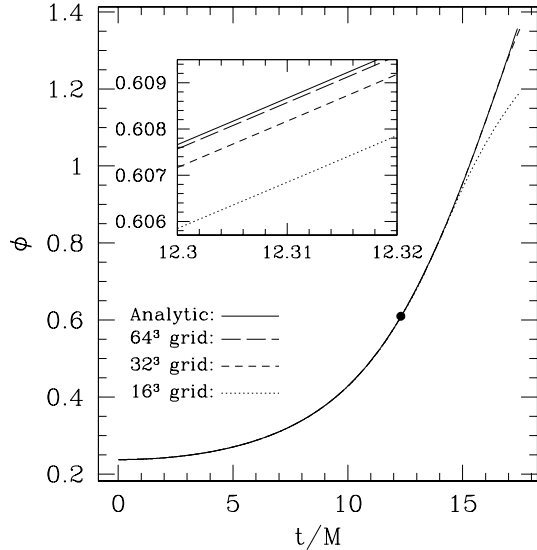


FIG. 4. Evolution of ϕ at the center for different grid resolutions for OS dust collapse to a black hole. We hold the outer boundary fixed at $x = y = z = 4M$ for each case. The dot indicates the time by which all the matter has passed inside the event horizon; the inset is a blow-up of the curve at that time. The numerical evolution follows the dynamical collapse well beyond black hole formation.

transverse fields and from the Ricci tensor, which contains second derivatives of the fields. This reduces errors in the longitudinal fields that arise from the discontinuous surface, highlighting the advantages of a conformal splitting.

In summary, we find that the system of equations described in paper I accurately evolves gravitational fields associated with matter sources. We can evolve the fields of an Oppenheimer-Volkoff star to extremely late times with harmonic slicing, and we can follow Oppenheimer-Snyder collapse well beyond black hole formation into the very strong-field regime. We used predetermined matter sources, and have decoupled the field evolution from hydrodynamic evolution — hydro without hydro.

Our findings have two important consequences. First, the ability to stably evolve the gravitational fields in the presence of strong-field matter sources is an important step towards constructing fully self-consistent, relativistic hydrodynamical codes. Second, our tests demonstrate that there are no fundamental difficulties evolving the fields with prescribed matter sources obeying $\nabla \cdot \mathbf{T} = 0$, rather than self-consistently evolving the matter and fields together. This hydro-without-hydro approach suggests a possible successive approximation scheme for calculating the gravitational-wave signal emitted by, for example, binary neutron stars. Outside the innermost stable circular orbit, such binaries are dominated by longitudinal fields and change their radial separation on a radiative timescale which is much longer

than the orbital timescale. They therefore may be considered in quasi-equilibrium (see, *e.g.*, [16]). Instead of evolving the matter hydrodynamically, we can insert the known quasi-equilibrium binary configuration into the field evolution code to get the transverse wave components approximately. Decreasing the orbital separation (and increasing the binding energy) at the rate found for the outflow of gravitational-wave energy would generate an approximate strong-field wave inspiral pattern. Such a hydro-without-hydro calculation may yield an approximate gravitational waveform from inspiraling neutron stars without having to couple the matter and field integrations.

We thank M. Shibata and S. Teukolsky for useful discussions. Calculations were performed on SGI CRAY Origin2000 computer systems at the National Center for Supercomputing Applications, University of Illinois at Urbana-Champaign. This work was supported by NSF Grant AST 96-18524 and NASA Grant NAG 5-3420 at Illinois.

-
- [1] K. Thorne, in *Proceedings of the Seventeenth Texas Symposium on Relativistic Astrophysics and Cosmology*, edited by H. Böhringer, G. E. Morfill and J. E. Trümper (Annals of the New York Academy of Sciences, Vol. 759, New York, 1995).
 - [2] Information about the Binary Black Hole Grand Challenge can be found at www.npac.syr.edu/projects/bh/, and about the Binary Neutron Star Grand Challenge at jean-luc.ncsa.uiuc.edu/nsnsgc/ and wugrav.wustl.edu/Relativ/nsgc.html.
 - [3] K. Oohara and T. Nakamura, in *Relativistic Gravitation and Gravitational Radiation*, edited by J.-A. Marck and J.-P. Lasota (Cambridge University Press, Cambridge, 1997).
 - [4] J. R. Wilson and G. J. Mathews, *Phys. Rev. Lett.* **75**, 4161 (1995); J. R. Wilson, G. J. Mathews and P. Maronetti, *Phys. Rev. D* **54**, 1317 (1996).
 - [5] R. Arnowitt, S. Deser and C. W. Misner, in *Gravitation: An Introduction to Current Research*, edited by L. Witten (Wiley, New York, 1962).
 - [6] A. M. Abrahams *et al.* (The Binary Black Hole Grand Challenge Alliance) *Phys. Rev. Lett.* **80**, 1812 (1998);
 - [7] S. Frittelli and O. Reula, *Commun. Math. Phys.* **166**, 221 (1994); C. Bona, J. Massó, E. Seidel and J. Stela, *Phys. Rev. Lett.* **75**, 600 (1995); A. Abrahams, A. Anderson, Y. Choquet-Bruhat and J. W. York, Jr., *Phys. Rev. Lett.* **75**, 3377 (1996); M. H. P. M. van Putten and D. M. Eardley, *Phys. Rev. D* **53**, 3056 (1996); H. Friedrich, *Class. Quantum Gravit.* **13**, 1451 (1996); A. Anderson, Y. Choquet-Bruhat and J. W. York, Jr., to appear in *Topol. Methods in Nonlinear Analysis* (also gr-qc/9710041); A. Anderson and J. W. York, Jr., submitted (also gr-qc/9901021).

- [8] M. A. Scheel, T. W. Baumgarte, G. B. Cook, S. L. Shapiro and S. A. Teukolsky, Phys. Rev. D **56**, 6320 (1997); Phys. Rev. D **58**, 044020 (1998).
- [9] C. Bona, J. Masso, E. Seidel and P. Walker, submitted (1998) (see also gr-qc/9804059).
- [10] T. W. Baumgarte and S. L. Shapiro, Phys. Rev. D **59**, 024007 (1999) (paper I).
- [11] M. Shibata and T. Nakamura, Phys. Rev. D **52**, 5428 (1995).
- [12] J. R. Oppenheimer and G. Volkoff, Phys. Rev **55**, 374 (1939).
- [13] J. R. Oppenheimer and H. Snyder, Phys. Rev **56**, 455 (1939).
- [14] J. A. Font, M. Miller, W.-M. Suen, M. Tobias, gr-qc/9811015.
- [15] L. I. Petrich, S. L. Shapiro and S. A. Teukolsky, Phys. Rev. D **31**, 2459 (1985).
- [16] T. W. Baumgarte, G. B. Cook, M. A. Scheel, S. L. Shapiro and S. A. Teukolsky, Phys. Rev. Lett. **79**, 1182 (1997); Phys. Rev. D **57**, 6181 (1998); Phys. Rev. D **57**, 7292 (1998).